Particle-like solutions to the Yang–Mills-dilaton system in $d = 4 + 1$ dimensions

Eugen Radu[†], Ya. Shnir[‡] and D. H. Tchrakian[†⋆]

[†]Department of Mathematical Physics, National University of Ireland Maynooth, Maynooth, Ireland

[‡]Institut für Physik, Universität Oldenburg, Postfach 2503 D-26111 Oldenburg, Germany

[⋆]School of Theoretical Physics – DIAS, 10 Burlington Road, Dublin 4, Ireland

December 8, 2006

Abstract

We construct static solutions to a $SU(2)$ Yang–Mills (YM) dilaton model in $4+1$ dimensions subject to bi-azimuthal symmetry. The YM sector of the model consists of the usual YM term and the next higher order term of the YM hierarchy, which is required by the scaling condition for the existence of finite energy solutions. The basic features of two different types of configurations are studied, corresponding to (multi)solitons with topological charge n^2, and soliton–antisoliton pairs with zero topological charge.

1 Introduction

Multi-instantons and composite instanton-antiinstanton bound states subject to bi-azimuthal symmetry were reported in a recent paper [1]. These were constructed numerically, for the usual ($p = 1$) $SU(2)$ Yang-Mills (YM) system in 4 Euclidean dimensions, the spherically symmetric special case being the usual BPST [2] instanton.

In a work [3] unrelated to [1], regular and black hole static and spherically symmetric solutions to a Einstein–YM (EYM) system in $4+1$ dimensional spacetime were constructed numerically. The YM system in that model had gauge group $SO(4)$, with the connection taking its values in (one of the two) chiral spinor representations of $SO(4)$, namely in $SU(2)$. Given that the solutions in [3] were static, *i.e.* that the YM field is defined on a 4 dimensional Euclidean space, the $SU(2)$ YM field in [3] is the same one as that in [1]. This is the relation between the two works [1] and [3], and our intention here is to exploit this relation.

The present work serves two distinct purposes. The first and main purpose is to pave the way for the construction of more general, non-spherically symmetric solutions to EYM systems in a five dimensional spacetime. To our knowledge, no such results in EYM theory have appeared in the literature to date. Although considerable progress has been made in constructing asymptotically flat higher dimensional EYM solutions[1] all known configurations were subject to spherical symmetry. Our choice of a YM-dilaton (YMd) model is made because it has been shown that, at least in $d = 3+1$ dimensions, the classical solutions of this system mimic the corresponding EYM solutions [9], so the dilaton–YM exercise serves as a warmup for the considerably more complex gravitational problem.

Concerning our particular choice of $4 + 1$ spacetime dimensions here, our reasons are: When imposing axial symmetry on a YM field in $d = D + 1$ dimensions the simplest way is, following [10], to impose spherical symmetry in the $D - 1$ dimensional subspace of the d spacelike dimensions. In this case the Chern-Pontryagin topological charge is fixed by the boundary conditions imposed on the first polar angle, and no analogue of the vortex number appearing in the axially symmetric Ansatz for $d = 3$ [11] is featured [10]. Technically, the absence of a vortex number makes the numerical integration much harder. Imposing axial symmetry in turns in the $x - y$ and $z - u$ planes of $D = 4$ Euclidean space as in [1] on the other hand, features two (equal) vortex numbers, making the numerical work technically more accessible. It is our intention to use the particular bi-azimuthally symmetric Ansatz of [1] in $D = 4$ that has led us to restrict ourselves to $d = 4 + 1$ dimensional spacetime. (Numerical work on implementing axial symmetry like in [10] is at present in active progress.) Of course, the exploitation of this type of symmetry is not restricted to $4 + 1$ spacetime, but can be extended to any odd $2q + 1$ spacetime where q distinct azimuthal symmetries are imposed, but this in practice results in residual PDE's of order three and higher for $q \geq 3$.

The second and subsidiary aim of this work is to break the scale invariance of the usual YM system in $D = 4$ studied in [1], and the introduction of the dilaton field does just that. The question of instanton–antiinstanton bound states in a scale breaking model is an interesing enough matter in itself, presenting a second important motivation for this work.

In Section 2 we present the model, impose the symmetry and state the boundary conditions, in successive subsections. The numerical results are presented in Section 3, presenting both solutions with spherical and bi-azimuthal symmetry. We give our conclusions and remarks in the final section.

[1] EYM particle-like and black hole solutions approaching at infinity the Minkowski background have been constructed numerically for $d = 6, 7$ and 8 [4]. The properties of globally regular solutions in arbitrary dimensions have been studied both numerically and analytically in [5]. Higher dimensional asymptotically (anti-)de Sitter solutions have been found numerically in [6], [7], as well as such systems whose gravitational sector consists of higher order Gauss-Bonnet like gravitational terms [8].

2 The model

The model in 5 spacetime dimensions with coordinates $x_M = (x_0, x_\mu)$ that we study here is described by the Lagrangian

$$\mathcal{L}_m = \frac{1}{4\pi^2}\left(|\partial_M\phi|^2 + \left(\frac{\tau_1}{2\cdot 2!}\,\mathrm{e}^{2a\phi}\,\mathrm{Tr}\,\mathcal{F}_{MN}^2 + \frac{\tau_2}{2\cdot 4!}\,\mathrm{e}^{6a\phi}\,\mathrm{Tr}\,\mathcal{F}_{MNRS}^2\right)\right) \tag{1}$$

where ϕ is the dilaton field, $\mathcal{F}_{MN} = \partial_M\mathcal{A}_N - \partial_N\mathcal{A}_M + [\mathcal{A}_M, \mathcal{A}_N]$ is the 2-form YM curvature and $\mathcal{F}_{MNRS} = \{\mathcal{F}_{M[N}, \mathcal{F}_{RS]}\}$ is the 4-form YM curvature consisting of the totally antisymmetrised product of two YM 2-form YM curvatures. (The bracket $[\nu\rho\sigma]$ implies cyclic symmetry.) τ_1 and τ_2 are dimensionful coupling strengths which will eventually be scaled out against the constant a in the exponent, which has the inverse dimension of the dilaton field ϕ. Similar to the $d = 3+1$ case, the form we choose for the coupling of the dilaton field to the nonabelian matter was found by requiring that a shift $\phi \to \phi + \phi_0$ of the dilaton field to be compensated by a suitable rescaling of the coordinates.

The YM sector of the action density in $4+1$ dimensions employed here, is that one used in [3], namely the superposed $p = 1$ and $p = 2$ members of the YM hierarchy[2]. The dilaton breaks the scale invariance of the usual $p = 1$ YM system, and a simple Derrick-type scaling argument shows that no finite mass/energy solution can exist if $\tau_2 = 0$, *i.e.* the $p = 2$ term in (1) is necessary.

The YM and dilaton field equations read

$$\tau_1 D_\mu\left(\mathrm{e}^{2a\phi}F^{\mu\nu}\right) + \frac{1}{2}\tau_2\{F_{\rho\sigma}, D_\mu\left(e^{6a\phi}\ F^{\mu\nu\rho\sigma}\right)\} = 0, \tag{2}$$

$$\nabla^2\phi = \frac{a}{2\pi^2}\left(2e^{2a\phi}\hat{L}_1 + 6e^{6a\phi}\hat{L}_2\right). \tag{3}$$

In (3) we have used the notation

$$\hat{L}_1 = \frac{\tau_1}{2\cdot 2!}\mathrm{Tr}\,\mathcal{F}_{MN}^2 \quad , \quad \hat{L}_2 = \frac{\tau_2}{2\cdot 4!}\mathrm{Tr}\,\mathcal{F}_{MNRS}^2\,. \tag{4}$$

2.1 Imposition of symmetry and residual action

In the YM connection $\mathcal{A}_M = (\mathcal{A}_0, \mathcal{A}_\mu)$, we choose the temporal component $\mathcal{A}_0 = 0$ to vanish and the spacelike components $\mathcal{A}_\mu$ is subjected to two successive axial symmetries, described in [1]. We denote the Euclidean four dimensional coordinates as $x_\mu = (x, y; z, u) \equiv (x_\alpha; x_i)$, with $\alpha = 1, 2$ and $i = 3, 4$, and use the following parametrisation

$$x_\alpha = r\sin\theta\,\hat{x}_\alpha \equiv \rho\,\hat{x}_\alpha, \quad x_i = r\cos\theta\,\hat{x}_i \equiv \sigma\hat{x}_i\,, \tag{5}$$

where $r^2 = |x_\mu|^2 = |x_\alpha|^2 + |x_i|^2$, with the unit vectors appearing in (5) parametrised as $\hat{x}_\alpha = (\cos\varphi_1, \sin\varphi_1)$, $\hat{x}_i = (\cos\varphi_2, \sin\varphi_2)$, with $0 \le \theta \le \frac{\pi}{2}$ spanning the quarter plane,

[2]The YM hierarchy labeled by the integer p was introduced in [12] in the context of self-dual solutions in $4p$ Euclidean dimensions, but superpositions of various p members were employed ubiquitously since.

and the two azimuthal angles $0 \leq \varphi_1 \leq 2\pi$ and $0 \leq \varphi_2 \leq 2\pi$. The $d = 4 + 1$ Minkowski spacetime metric reads for this ansatz

$$ds^2 = -dt^2 + dr^2 + r^2(d\theta^2 + \sin^2\theta d\varphi_1^2 + \cos^2\theta d\varphi_2^2). \tag{6}$$

The first stage of symmetry imposition is of cylindrical symmetry in the $x_\alpha = (x_1, x_2)$ plane, and the Ansatz is stated as is

$$\mathcal{A}_\alpha = \left(\tfrac{\phi^5 + n_1}{\rho}\right) \Sigma_{\alpha\beta}\hat{x}_\beta + \left(\tfrac{\phi^m}{\rho}\right) (\varepsilon\hat{x})_\alpha \, (\varepsilon n^{(1)})_\beta \, \Sigma_{\beta m} + A_\rho^{m5} \, \hat{x}_\alpha n_\beta^{(1)} \, \Sigma_{\beta m} - A_\rho^{34} \, \hat{x}_\alpha \Sigma_{34} \ , \tag{7}$$

$$\mathcal{A}_i = A_i^{m5} \, n_\beta^{(1)} \, \Sigma_{\beta m} - A_i^{34} \, \Sigma_{34} \ , \tag{8}$$

in which the index $m = 3, 4$ is summed over, and the unit vector $n_\alpha^{(1)} = (\cos n_1\varphi_1 \, , \, \sin n_1\varphi_1)$ is labeled by the vortex integer n_1, $\varepsilon_{\alpha\beta}$ being the Levi-Civita symbol. The spin matrices $\Sigma_{\mu\nu} = (\Sigma_{\alpha\beta}, \Sigma_{\alpha i}, \Sigma_{ij})$ in (7) and (8) are one or other of the two chiral representations of $SO(4)$, *i.e.* they are $SU(2)$ matrices.

If in (7)-(8) we regard the functions $(\phi^m, \phi^5) \equiv \phi^a$ as a $SO(3)$ isovector field, and $(A_\rho^{m5}, A_\rho^{34}) \equiv A_\rho^{ab}$ and $(A_i^{m5}, A_\rho^{34}) \equiv A_i^{ab}$ as $SO(3)$ YM connection fields, with antisymmetric $SO(3)$ algebra indices $[ab] = ([34], [45], [53]$, then it turns out that $\mathcal{F}_{\mu\nu} = (\mathcal{F}_{\alpha\beta}, \mathcal{F}_{\alpha i}, \mathcal{F}_{ij})$ is expressed exclusively in terms of the curvature $(F_{ij}^{ab}, F_{i\rho}^{ab})$ of the $SO(3)$ connection (A_ρ^{ab}, A_i^{ab}), and the corresponding covariant derivative $(D_i\phi^a, D_\rho\phi^a)$ of ϕ^a, all defined on the hyperbolic space with coordinates (x_i, x_ρ).

The second stage of symmetry imposition is expressed most succintly by rewriting the residual fields (A_i^{ab}, A_ρ^{ab}) and ϕ^a on this hyperbolic space in matrix representation

$$A_i = -\frac{1}{2} \, A_i^{ab} \, \Sigma_{ab} \qquad , \qquad A_\rho = -\frac{1}{2} \, A_\rho^{ab} \, \Sigma_{ab} \ , \tag{9}$$

$$\Phi \ = \ \phi^a \, \Sigma_{a4} \, . \tag{10}$$

Azimutal symmetry in the $(x_3 - x_4)$ plane is imposed on the connection fields (9) by decomposing A_i formally according to (7) and A_ρ according to (8). Noticing now that the index a in (9)-(10) runs only over three values, and reassigning the values of the index $i = 1, 2$, the analogues of (7) and (8) contract to give

$$A_i \ = \ \left(\frac{\chi^4 + n_2}{\sigma}\right) \Sigma_{ij}\hat{x}_j + \left(\frac{\chi^3}{\rho}\right) (\varepsilon\hat{x})_i \, (\varepsilon n^{(2)})_j \, \Sigma_{j3} + A_\sigma^{34} \ \hat{x}_i n_j^{(2)} \, \Sigma_{j3} \ , \tag{11}$$

$$\mathcal{A}_\rho \ = \ A_\sigma^{34} \, n_j^{(2)} \, \Sigma_{jm} \ , \tag{12}$$

exhibiting the Abelian connection A_σ^{34} analogous to the Abelian connection A_ρ^{34} appearing in (7) and the isodoublet function (χ^3, χ^4).

The corresponding axially symmetric decomposition of Φ in (10) is

$$\Phi = \xi^1 \, n_j^{(2)} \, \Sigma_{j4} + \xi^2 \, \Sigma_{34} \, . \tag{13}$$

In (11)-(12) and (13) we have used the unit vector $n_i^{(2)} = (\cos n_2\varphi_2 \, , \, \sin n_2\varphi_2)$, with vorticity integer n_2. The final stage of symmetry imposition is to treat the two azimuthal symmetries

imposed in the $x-y$ and the $z-u$ planes on the same footing, leading to the equality of the two vortex numbers, $n_1 = n_2 \equiv n$.

Denoting the residual functions $(A^{34}_\rho, A^{34}_\sigma) = (a_\rho a_\sigma,)$, $(\chi^3, \chi^4) = \chi^A$, $(\xi^1, \xi^2) = \xi^A$, and regarding (a_ρ, a_σ) as an Abelian connection on the quater plane defined by (ρ, σ), the residual action densities can be expressed exclusively in terms of the $SO(2)$ curvature

$$f_{\rho\sigma} = \partial_\rho a_\sigma - \partial_\sigma a_\rho \tag{14}$$

and the covariant derivatives

$$\begin{aligned} \mathcal{D}_\rho \chi^A = \partial_\rho \chi^A + a_\rho (\varepsilon\chi)^A \quad , \quad \mathcal{D}_\sigma \chi^A = \partial_\sigma \chi^A + a_\sigma (\varepsilon\chi)^A, \\ \mathcal{D}_\rho \xi^A = \partial_\rho \xi^A + a_\rho (\varepsilon\xi)^A \quad , \quad \mathcal{D}_\sigma \xi^A = \partial_\sigma \xi^A + a_\sigma (\varepsilon\xi)^A. \end{aligned} \tag{15}$$

The residual one dimensional YM action densities descending from the $p=1$ and the $p=2$ terms $\hat{L}_1$ and $\hat{L}_2$ defined by (4) are, respectively,

$$\begin{aligned} L_1 &= \frac{\tau_1}{4}\left[\rho\sigma\, f^2_{\rho\sigma} + \frac{\rho}{\sigma}\left(|\mathcal{D}_\rho\chi^A|^2 + |\mathcal{D}_\sigma\chi^A|^2\right) + \frac{\sigma}{\rho}\left(|\mathcal{D}_\rho\xi^A|^2 + |\mathcal{D}_\sigma\xi^A|^2\right) + \frac{1}{\rho\sigma}(\varepsilon^{AB}\chi^A\xi^B)^2\right], \\ L_2 &= \frac{\tau_2}{12\,\rho\sigma}\left(\varepsilon_{AB}\chi^A\xi^B\, f_{\rho\sigma} + \mathcal{D}_{[\rho}\chi^A\,\mathcal{D}_{\sigma]}\xi^A\right)^2. \end{aligned} \tag{16}$$

These residual action densities are scalars with respect to the *local* $SO(2)$ indices A, B, hence they are manifestly gauge invariant. They describes a $U(1)$ Higgs like model with **two** effective Higgs fields χ^A and ξ^A, coupled minimally to the $U(1)$ gauge connection (a_ρ, a_σ). To remove this $U(1)$ gauge freedom we impose the usual gauge condition

$$\partial_\rho a_\rho + \partial_\sigma a_\sigma = 0\ . \tag{17}$$

Since our numerical constructions will be carried out using the coordinates (r, θ) we display (16) also as

$$\begin{aligned} L_1 &= \frac{\tau_1}{4}\Bigg[r\sin\theta\cos\theta\, f^2_{r\theta} + \frac{r\sin\theta}{\cos\theta}\left(|\mathcal{D}_r\chi^A|^2 + \frac{1}{r^2}|\mathcal{D}_\theta\chi^A|^2\right) \\ &\qquad + \frac{r\cos\theta}{\sin\theta}\left(|\mathcal{D}_r\xi^A|^2 + \frac{1}{r^2}|\mathcal{D}_\theta\xi^A|^2\right) + \frac{1}{r\sin\theta\cos\theta}(\varepsilon^{AB}\chi^A\xi^B)^2\Bigg] \qquad (18) \\ L_2 &= \frac{\tau_2}{12\, r^3\,\sin\theta\cos\theta}\left(\varepsilon_{AB}\chi^A\xi^B f_{r\theta} + \mathcal{D}_{[r}\chi^A\mathcal{D}_{\theta]}\xi^A\right)^2\ . \qquad (19) \end{aligned}$$

The total mass-energy M of the system is

$$M = \int d^4x\sqrt{g}\ \mathcal{L}_m = \int_0^\infty dr \int_0^{\pi/2} d\theta\ \left[\frac{1}{2}r^3\sin\theta\cos\theta(\phi^2_{,r} + \frac{1}{r^2}\phi^2_{,\theta}) + (e^{2a\phi}L_1 + e^{6a\phi}L_2)\right], \tag{20}$$

and equals the total action of solutions, viewed as solitons in a $d=4$ Euclidean space.

2.2 Boundary conditions

To obtain regular solutions with finite energy density we impose at the origin ($r = 0$) the boundary conditions

$$a_r = 0 \quad , \quad a_\theta = 0 \quad , \quad \chi^A = \begin{pmatrix} 0 \\ -n_2 \end{pmatrix} \quad , \quad \xi^A = \begin{pmatrix} 0 \\ -n_1 \end{pmatrix} \ , \tag{21}$$

which are requested by the analyticity of the YM ansatz, and $\partial_r \phi|_{r=0} = 0$ for the dilaton field. In order to find finite mass solutions, we impose at infinity

$$a_r = 0,\ a_\theta = -2m,\ \chi^A = (-1)^{m+1} n_2 \begin{pmatrix} \sin 2m\theta \\ \cos 2m\theta \end{pmatrix},\ \xi^A = -n_1 \begin{pmatrix} \sin 2m\theta \\ \cos 2m\theta \end{pmatrix},\ \phi = 0, \tag{22}$$

m being a positive integer. Similar considerations lead to the following boundary conditions on the ρ and σ axes:

$$a_r = \frac{1}{n_1}\partial_r \xi^1,\ \ a_\theta = \frac{1}{n_1}\partial_\theta \xi^1,\ \ \chi^1 = 0,\ \ \xi^1 = 0,\ \ \partial_\theta \chi^2 = 0,\ \ \xi^2 = -n_1,\ \partial_\theta \phi = 0, \tag{23}$$

for $\theta = 0$, and

$$a_r = \frac{1}{n_2}\partial_r \chi^1,\ \ a_\theta = \frac{1}{n_2}\partial_\theta \chi^1,\ \ \chi^1 = 0,\ \ \xi^1 = 0,\ \ \chi^2 = -n_2,\ \ \partial_\theta \xi^2 = 0,\ \ \partial_\theta \phi = 0, \tag{24}$$

for $\theta = \pi/2$, respectively.

2.3 Topological charge

In our normalisation, the topological charge is defined as

$$q = \frac{1}{32\pi^2}\varepsilon_{\mu\nu\rho\sigma} \int \mathrm{Tr}\{\mathcal{F}_{\mu\nu}\mathcal{F}_{\rho\sigma}\}\, d^4x\,, \tag{25}$$

which after integration of the azimuthal angles (φ_1, φ_2) reduces to

$$q = \frac{1}{2}\varepsilon_{\mu\nu} \int \left(\frac{1}{2}\,\varepsilon_{AB}\chi^A \xi^B\, f_{\mu\nu} + \mathcal{D}_\mu \chi^A\, \mathcal{D}_\nu \xi^A \right) d^2x \tag{26}$$

$$= \frac{1}{4} \int \varepsilon_{\mu\nu}\, \partial_\mu (\chi^A \mathcal{D}_\nu \xi^A - \xi^A \mathcal{D}_\nu \chi^A)\, d^2x\,. \tag{27}$$

The integration in (26) is carried out over the 2 dimensional space $x_\mu = (x_\rho, x_\sigma)$. As expected this is a total divergence expressed by (27).

Using Stokes' theorem, the two dimensional integral of (27) reduces to the one dimensional line integral

$$q = \frac{1}{4} \int \chi^A \overset{\leftrightarrow}{\mathcal{D}}_\mu \xi^A\, ds_\mu, \tag{28}$$

This integral has been evaluated in [1] by reading off the appropriate values of χ^A and ξ^A from (23)-(24). The result is

$$q = \frac{1}{2}\,[1 - (-1)^m] n_1 n_2. \tag{29}$$

3 Numerical results

Apart from the coupling constants τ_1 and τ_2 the model contains also the dilaton constant a. Dimensionless quantities are obtained by rescaling

$$\phi \to \phi/a, \quad r \to r(\tau_2/\tau_1)^{1/4}, \tag{30}$$

This reveals the existence of one fundamental parameter which gives the strength of the dilaton-nonabelian interaction

$$\alpha^2 = a^2 \tau_1^{3/2}/\tau_2^{1/2}\,, \tag{31}$$

which is a feature present also in the EYM case [3]. We use this rescaling to set $\tau_1 = 1$, $\tau_2 = 1/3$ in the numerical computation, without any loss of generality.

One can see that the limit $\alpha \to 0$ can be approached in two ways and two different branches of solutions may exist. The first limit corresponds to a pure $p = 1$ YM theory with vanishing dilaton and $p = 2$ YM terms, the solutions here replicating the (multi-)instantons and composite instanton-antiinstanton bound states discussed in [1]. The other possibility corresponds to a finite value of the dilaton coupling a as $\tau_1 \to 0$. Thus, the second limiting configuration is a solution of the truncated $p = 2$ YM system interacting with the dilaton, with no $p = 1$ YM term.

We have studied YMd solutions with $m = 1,\ 2$. From our knowledge of the tolopogical charges (29), the $m = 1$ solutions will describe (multi)solitons and the $m = 2$ solutions, soliton-antisoliton configurations. Also, to simplify the general picture we set $n_1 = n_2 = n$ in the boundary conditions (21)-(24).

The spherically symmetric solutions are found by using a standard differential equations solver. The numerical calculations in the bi-azimuthally symmetric case were performed with the software package CADSOL, based on the Newton-Raphson method [13]. In this case, the field equations are first discretized on a nonequidistant grid and the resulting system is solved iteratively until convergence is achieved. In this scheme, a new radial variable $x = r/(1 + r)$ is introduced which maps the semi-infinite region $[0, \infty)$ to the closed region $[0, 1]$.

As will be described below, solutions exist for certain ranges of the parameter α. It turns out that $m = 1$ solutions with all n and $m = 2$ solutions with $n = 1$ exist for a range of α starting from a $\alpha \to 0$ limit, but do not persist all the way up to the second $\alpha \to 0$ limit. (However, the way the solutions approach the limit $\alpha \to 0$ depends on m.) By contrast we find that $m = 2$ solutions with all $n > 1$, exist for all α between the two limits.

3.1 $m = 1$ configurations

$n = 1$ spherically symmetric solutions

In the spherically symmetric limit, which case we shall analyse numerically first, the angular dependence of these functions is fixed and the only remaining independent function depends

on the variable r. The independent function in this case is $a_\theta = w(r)-1$, with the remaining fuctions (a_r, χ^A, ξ^A) given by

$$a_r = 0,\ \chi^1 = -\xi^1 = \frac{1}{2}(w(r)-1)\sin 2\theta,\ \ \chi^2 = -(w(r)-1)\cos^2\theta - 1,\ \ \xi^2 = -(w(r)-1)\sin^2\theta - 1. \tag{32}$$

The functions $\phi(r)$ and $w(r)$ satisfy the equations

$$(r^3\phi')' = \alpha^2\left(2e^{2\phi}\tau_1(rw'^2 + \frac{(w^2-1)^2}{r}) + 9e^{6\phi}\tau_2\frac{(w^2-1)^2}{r^3}w'^2\right),$$
$$\left(e^{2\phi}rw'(\tau_1 + 3e^{4\phi}\tau_2\frac{(w^2-1)^2}{r^4})\right)' = \frac{2e^{2\phi}w(w^2-1)}{r}\left(\tau_1 + 3\tau_2 e^{4\phi}\frac{w'^2}{r^2}\right). \tag{33}$$

The asymptotic solutions to these functions can be systematically constructed in both regions, near the origin and for $r \gg 1$. The small r expansion is

$$w(r) = 1 - br^2 + O(r^4),\quad \phi = \phi_0 + 4\alpha^2(\frac{\tau_1}{2} + 9\tau_2 b^2)b^2r^2 + O(r^4), \tag{34}$$

with b, ϕ_0 two real parameters, while as $r \to \infty$ we find

$$w(r) = \pm 1 - \frac{4\phi_1}{r^2} - \frac{4\phi_1^3}{27r^6} + O(1/r^8),\quad \phi = \frac{\phi_1}{r^2} - \frac{32\alpha^2\phi^3 e^{2\phi_0}\tau_1}{27r^6} + O(1/r^8). \tag{35}$$

We numerically integrate the Eqs. (33) with the above set of boundary conditions for $\tau_1 = 1, \tau_2 = 1/3$ and varying α. The picture we found is very similar to that found for the EYM system [3], the dilaton coupling constant playing the role of the Newton constant. First, for a given α, solutions with the right asymptotics exist for a single value of the "shooting" parameter b which enters the expansion (34). For α small enough, a branch of solutions smoothly emerges from the BPST configuration [2]. When α increases, the mass M and the absolute value of the dilaton function at the origin increase, as indicated in Figure 1. These solutions exist up to a maximal value $\alpha_{max} \simeq 0.36928$ of the parameter α.

As in the corresponding gravitating case [3], we found another branch of solutions in the interval $\alpha \in [\alpha_{cr(1)}, \alpha_{max}]$ with $\alpha^2_{cr(1)} \simeq 0.2653$. On this second branch of solutions, both $\phi(0)$ and M continue to increase but stay finite. However, a third branch of solutions exists for $\alpha \in [0.2653, 0.2652]$, on which the two quantities increase further. A fourth branch of solutions has also been found, with a corresponding $\alpha_{cr(3)} \simeq 0.2642$. The mass M, the value of the dilaton field at the origin $\phi(0)$ and the initial (shooting) parameter b increase along these branches. Further branches of solutions, exhibiting more oscillations around $\alpha \simeq 0.264$ are very likely to exist but their study is a difficult numerical problem. This critical behaviour is described as a *conical fixed point* in the analytic analysis in [5]. Therefore we conclude that, as in the spherically symmetric gravitating case [3], the limit $\tau_1 = 0$ is not approached for solutions with $m = 1,\ n = 1$.

As a general feature, all solutions discussed here present only one node in the gauge function $w(r)$. As in the higher dimensional EYM models discussed in [4, 5], no multinode solutions were found.

$n > 1$

Solutions with bi-azimuthal symmetry with nontrivial dependence on both r and θ are found for $(n_1, n_2) \neq 1$ subject to the boundary conditions (21)-(24). We have studied solutions for $m = 1$ with $2 \leq n \leq 5$. The general features of the $m = 1$ solutions are the same for all $n > 1$. Also, as seen in (29), the $m = 1$ configurations carry a topological charge $q = n^2$. The corresponding solutions of the $\mathcal{F}^2_{MN}$ model are self-dual and have been considered already in [14], [15] (for a different parametrization of the gauge field, however).

These solutions are constructed by starting with the known spherically symmetric configuration and increasing the winding number n in small steps. The iterations converge, and repeating the procedure one obtains in this way solutions for arbitrary n. The physical values of n are integers. The typical numerical error for the functions is estimated to be of the order of 10^{-3} or lower.

Any spherically symmetric configuration appears to result in generalisations with higher winding numbers n. Moreover, the branch structure noticed for the $m = 1,\ n = 1$ case seems to be retained by the higher winding number $m = 1$ solutions. Again, the first branch of solutions exists up to a maximal value of α, where another branch emerges, extending backwards in α. We managed to construct higher winding number n counterparts of the first two branches of spherically symmetric solutions. The mass M and the absolute value of the dilaton function at the origin increase along these branches, as shown in Figure 2. Note that the value of the dilaton function at the origin exhibited in the figures is actually $\phi(r = 0, \theta = 0)$, restricting to $\theta = 0$. This restriction is reasonable since for all solutions with bi-azimuthal symmetry discussed in this paper, the dilaton function at $r = 0$ presents almost no dependence on the angle θ.

We expect that the oscillatory pattern of $\phi(0)$ arising from the *conical fixed point* observed above for the spherically symmetric $n = 1$ solutions, will also be discovered for the $n > 1$ solutions here, but their construction is a difficult numerical problem beyond the scope of the present work.

In Figure 3 we present the gauge functions, the dilaton, and the topological charge density

$$\varrho = \frac{1}{4}\varepsilon_{\mu\nu}\ \left(\varepsilon_{AB}\chi^A\xi^B\, f_{\mu\nu} + \mathcal{D}_{[\mu}\chi^A\, \mathcal{D}_{\nu]}\xi^A\right)$$

read off (26), as functions of the radial coordinate r for five different angles for a typical first branch $m = 1,\ n = 3$ solution with $\alpha = 0.21$. The functions a_θ and ϕ have a small θ dependence (although the angular dependence increases with n), while χ_1 and ξ_1 have rather similar shapes. The action density $\mathcal{L}$ possesses one maximum on the $\theta = \pi/4$ axis. All multicharge solutions found have concentrated energy and charge density profiles where individual (unit) charge consituents do not appear as distinct components. The moduli of the effective Higgs fields $|\chi| = (\chi^A\chi^A)^{1/2}$ and $|\xi| = (\xi^A\xi^A)^{1/2}$ possess one node each on the ρ and the σ axes, respectively, which coincide with the maximum of the action density. The position of this node moves inward along the first and second branches.

3.2 $m = 2$ configurations

The $m = 2$ configurations can be thought of as composite systems consisting of two components which are pseudoparticles of topological charges $\pm n$. Thus, these configurations reside in the topologically trivial sector and carry no Chern-Pontryagin topological charge. This type of solutions have no spherically symmetric limit. Also, their behaviour as a function of α is different from those with $m = 1$ presented above, in that solutions for all values of α exist between the two distinct limits of $\alpha \to 0$ implied by (31), for all n except for $n = 1$.

$n = 1$

It is perhaps interesting to note from the outset that $m = 2$, $n = 1$ solutions to be described now, have apparently no counterpart in the $4 + 0$ dimensional $p = 1$ YM model studied in [1]. (It turns out that for the $(m = 2, n = 1)$ solution in that case there is no analytic proof of existence either.) The obvious difference of the $4 + 1$ dimensional model (1) here and the $4 + 0$ dimensional $p = 1$ YM model is that the solutions of the former are parametrised by the effective coupling constant α, while the latter has no such parameter. As will be described below, $m = 2$ $n = 1$ solutions exist for a certain range of α, and this range excludes the limiting case where the contribution to the action of the dilaton term and the $p = 2$ YM term in (1) disappear, *i.e.* a $\mathcal{F}^2_{MN}$ model.

We find that in the limit $\alpha \to 0$ resulting from $a \to 0$, *cf.* (31), no solutions of this type exist. However in the limit $\alpha \to 0$ corresponding to a finite value of the dilaton coupling a as $\tau_1 \to 0$, such solutions exist. This limiting configuration is then a solution of the truncated system consisting of the dilaton term and $p = 2$ YM term $\mathcal{F}^2_{MNRS}$, which dominate. Its characteristic feature is that for this configuration both nodes of the effective Higgs fields $|\chi|$ and $|\xi|$ merge on the $\theta = \pi/4$ axis. A family of solutions of the model (1) emerges from this configuration. As α increases, the nodes move towards the symmetry axes, ρ and σ, respectively, forming two identical vortex rings whose radii slowly decrease while the separation of both rings from the origin increase. At the critical value $\alpha_{cr} \simeq 0.265$ the node structure of the configuration changes, both vortex rings shrink to zero size and two isolated nodes appear on each symmetry axis. This structure is known for the usual YM system in $d = 4 + 0$ [1], indeed, increasing of α along this branch can be associated with increasing of the coupling τ_1 w.r.t. τ_2 as the dilaton coupling a remains fixed; then the term $\mathcal{F}^2_{MN}$ becomes leading. The maximum of the action density however is still located on $\theta = \pi/4$ axis.

Another similarity with the instanton-antiinstanton solution of the $d = 4+0$ $p = 1$ YM theory is that the gauge functions a_r, a_θ as well the dilaton function ϕ of the $n = 1, m = 2$ solutions also are almost θ-independent. Along this branch the mass of the solutions grows with increasing α since with increasing coupling τ_1 the contribution of the term $\mathcal{F}^2_{MN}$ also increases.

As the effective coupling increases further beyond α_{cr} the relative distance between the nodes increases, one lump moving towards the origin while the other one moves in the

opposite direction. Along this branch both the value of the dilaton field at the origin $|\phi(0)|$ and mass of configuration M increase as α increases. This branch extends up to a maximal value $\alpha^{(1)}_{max} \simeq 0.311$ beyond which the dilaton coupling becomes too strong for the static configuration to persist. The second branch, whose energy is higher, extends backwards up to $\alpha^{(2)}_{max} \simeq 0.279$. Along this branch both $|\phi(0)|$ and the mass of the configuration continue to increase as α decreases. Also the separation between the nodes decreases and both nodes invert direction of the motion, moving toward each other along this branch. In Figure 5 we present the values of the dilaton function at the origin $\phi(0)$ and the total mass (rescaled by α^2) of these configurations as functions of α.

$n = 2$

This configuration also resides in the topologically trivial sector and can be considered as consisting of two solitons of charges $n = \pm 2$. Then the interaction between the nonabelian matter fields becomes stronger than in the case of unit charge constituents and the expected pattern of possible branches of solutions is different from the $n = 1$ case above.

Indeed, the $n = 2$, $m = 2$ solutions show a different dependence on the coupling constant α, with two branches of solutions. The lower branch emerges from the corresponding solution in pure $p = 1$ YM theory with vanishing dilaton and $p = 2$ YM terms, replicating the corresponding solution in [1]. The variation of the effective coupling along this branch is associated with the decrease of τ_1, at fixed τ_2 and fixed dilaton coupling a. The second branch emerges from a solution of the $p = 2$ YM-dilaton system, the unrescaled mass M diverging in this limit, with the rescaled mass $M\alpha^2$ vanishing as seen from Figure 5a. At the maximal value $\alpha_{max} \simeq 0.2372$ this branch bifurcates with the lower YM branch. For larger values of α, the dilaton coupling becomes too strong for the static configurations to persist. Thus for $0 \leq \alpha < \alpha_{max}$ we notice the existence of (at least) two distinct solutions for the same value of coupling constant.

For the same value of α, the mass of the second branch solution is larger that that of the corresponding lower branch configuration(s). One should also notice the existence of a curious backbending of the lower branch for $0.193 < \alpha < 0.218$. Four distinct solutions exist in this case for the same value of α (three of them located on the lower branch), distinguished by the value of the mass and the dilaton field at the origin. This pattern is illustrated in Figure 5.

Again, observation of the positions and structure of the nodes of the effective scalar fields allows us to better understand the behaviour of the solutions. For lower branch solutions with small values of α there are two (double) nodes of the fields $|\chi|$ and $|\xi|$ on the ρ and σ symmetry axes respectively. The locations of nodes correspond to the locations of the two individual constituents and the action density distribution posesses two distinct maxima on the $\theta = \pi/4$ axis. The distance between these nodes changes only slightly along the lower mass branch. The backbending in α observed in this case is reflected also for in the relative positions of the nodes. At the maximal value of α, the inner node is located at $\rho^{(1)}_0 = \sigma^{(1)}_0 \simeq 2.97$ and the outer node is located at $\rho^{(2)}_0 = \sigma^{(2)}_0 \simeq 4.18$.

Along the upper branch, as α slightly decreases below α_{max}, the inner node inverts

direction of its movement toward the outer node which still moves inwards. Thus, both nodes on the symmetry axis rapidly approach each other and merge forming a two vortex ring solution as $\alpha \simeq 0.2355$. The action density then has a single maximum on $\theta = \pi/4$ axis. As α decreases further both nodes move away from the symmetry axis and their positions do not coincide with the location of the maximum of the action density. Further decreasing α results in the increase of the radii of the two rings around the symmetry axis, and in the limit $\alpha \to 0$ the rings touch each other on the $\theta = \pi/4$ axis.

In Figure 4 we give three dimensional plots of the modulus of the effective Higgs field ξ for the $n = m = 2$ upper branch vortex solution at $\alpha = 0.20$ and the $n = m = 2$ lower branch double node solution at the same value of α. The action density as given by (1) is also plotted at $\alpha = 0.20$ both for the upper and for the lower branches.

The numerical calculations indicate the possibility that the solutions of the fundamental YM branch, namely the branch on which the $p = 1$ YM term dominates, are not unique. It is possible that higher linking number configurations with higher masses might exist. This possibility will be explored elsewhere.

$n = 3$

For the $n = 3$ configuration composed of two triple charged pseudoparticles we observe a somewhat simpler pattern. The lower dilaton branch emerges from the limit of vanishing dilaton and $p = 2$ YM couplings and extends up to a maximal value $\alpha_{cr} = 0.165$. Along this branch the configuration posesses two vortex rings.

As α increases the mass of the solution increases and, at the same time, the radii of the rings slowly increase and both rings move inwards. This lower mass branch bifurcates at the critical value of the effective coupling α_{cr} with an upper branch which extends all the way back to $\alpha = 0$ (see Figure 5). Again, in this limit both vortex rings come into contact on the $\theta = \pi/4$ axis. Thus, we observe no isolated nodes on the symmetry axis and both upper and lower energy branches correspond to vortex ring solutions.

Note that the branch structure here closely resembles the pattern which was observed for the gravitating monopole-antimonopole chains and vortex solutions in $d = 3 + 1$ Einstein-Yang-Mills-Higgs system [16, 17].

The profiles of a typical $m = 2,\ n = 3$ solution are presented in Figure 6 (the picture there applies as well for $n = 1,\ 2$ configurations).

4 Summary and discussion

Finite mass static solutions to a $4 + 1$ dimensional $SU(2)$ YMd model are constructed numerically. The YM sector of the model consists of the usual YM term, labeled $p = 1$, and the next higher order $p = 2$ term of the YM hierarchy [12]. The second YM term is necessary to counteract the scaling of the dilaton term, since we require finite energy solutions. The solutions constructed are subject to the bi-azimuthal symmetry applied in [1].

Viewed as a $4+0$ dimensional model, this is a scale breaking version of a $p=1$ YM theory whose bi-azimuthally symmetric solutions were presented in [1]. The latter model being scale invariant in $d=4+0$, the present solutions have the new feature that they are referred to an absolute scale. This is an interesting feature of the present work.

Our main motivation here, however, is to study a system which can give an insight into the qualitative features of static, finite mass solutions to a gravitating YM system in higher dimensions, which are not subject to spherical symmetry. To date the only higher dimensional Einstein–Yang-Mills (EYM) solutions known [4, 3, 6, 5, 8] are subject to spherical symmetry in the spacelike dimensions. Rather than tackle the appreciably more complex numerical problem of constructing non spherically symmetric EYM solutions, we consider here instead the corresponding YM–dilaton problem, knowing that the classical solutions of the latter simulate [9] the qualitative properties of the corresponding EYM ones in $d=3+1$ dimensional spacetime. Thus the present work is a warmup to the ultimate aim of constructing non-spherically symmetric EYM solutions in higher dimensions. Having said that, we note that we have already made an appreciable start in the construction of the corresponding $d=4+1$ EYM solutions, and our results to date confirm the qualitative similarity of those with the dilaton–YM solutions presented here. Our results on the gravitating system will be reported elsewhere.

In the context of giving a qualitative description of our results, it must be noted that in this first effort, we have restricted the dimensionality of the spacetime to $4+1$. Thus we can only compare our results here with the $4+1$ dimensional subset of the spherically symmetric EYM solutions [4, 3, 6, 5, 8], which were given in spacetime dimensions $d \geq 5$. We would expect however that the comparative features between spherically and the non spherically symmetric solutions which we uncover here, will stay qualitatively valid also in dimensions $d \geq 5$.

As it happens, spherically symmetric EYM solutions in $4+1$ dimensions [3] exhibit quite different qualitative properties compared to those in $5+1$, $6+1$ and $7+1$ dimensions [4]. Indeed, the comparative patterns remain true modulo $4p$ dimensions, as explained in [5]. These features in question concern the branch structure of the said solutions with respect to the effective coupling parameter α in the problem. It turns out that for an appropriate EYM model in $d=4p+1$ dimensions, a peculiar branch structure, absent in $d \neq 4p+1$, occurs. This was explained in [5] to be due to the occurence of what was called there a *conical fixed point singularity*, which manifests itself by the oscillatory behaviour in α of the global quantities near the critical value of the effective coupling parameter[3].

Now in the present work we do not employ gravity but have instead the dilaton, which is represented by the singlet scalar field ϕ. It is therefore unavoidable that the role of the metric function at the origin in the gravitating case, should be replaced here by $\phi(r=0)$, the dilaton function at the origin. This correspondence can be made uniquely in the special case of our $(m=1\ ,\ n=1)$ bi-azimutal solutions, which are simply the spherically

[3] This feature persists also when a scalar matter field is added, for example when a gauged Grassmannian sigma model field is included in the Lagrangian [18]. We expect it to persists also when a Higgs field is added instead, in $4p+1$ dimensions.

symmetric subset. As seen from Figure 1, the oscillatory pattern of $\phi(0)$ is clear.

Concerning $(m \geq 2\ ,\ n)$ solutions, these are not spherically symmetric and depend on θ in addition to r. Instead we have employed the values $\phi(r = 0, \theta = 0)$ to track the branch behaviour of our solutions. This is quite a reasonable criterion, since we find that the dependence of $\phi(0, \theta)$ is very small on all branches constructed. The branch structures for $(m = 2\ ,\ n = 1, 2, 3)$ are displayed on Figure 5. We see that $(m = 2\ ,\ n = 2, 3)$ solutions have largely similar patterns, except for the additional backbending showing up in the $n = 2$ case. The branch structure for $(m = 2\ ,\ n = 1)$ on the other hand is drastically different. Indeed it seems quite reminiscent of the corresponding spherically symmetric $(m = 1\ ,\ n = 1)$ solutions, pehaps exhibiting a *conical fixed point* behaviour too, but the numerical accuracy is entirely inadequate to decide this, either way.

Our results concerning $m \geq 2$ solutions are here restricted to the concrete construction of $m = 2$ solutions. However, our preliminary numerical results indicate that most qualitative features remain true for $m = 3,\ 4$. Also, for $m = 2$, we have restricted to $n = 1, 2, 3$ only, which is quite adequate. An interesting remark on $m = 2$ solutions is the existence of the $(m = 2\ ,\ n = 1)$ confirmed by our results, which we had not found for the $d = 4 + 0$ dimensional $p = 1$ YM model in [1], and for which the analytic proof of existence is also absent. This is easy to understand since our $(m = 2\ ,\ n = 1)$ solutions exist only for that range of the parameter α for which all terms in the Lagrangian (1) contribute to the action, and for the limiting range of α for which only the usual YM term ($p = 1$ term) would dominate, there are no solutions. So there is no special case of our solutions which could describe $(m \geq 2\ ,\ n = 1)$ bi-azimuthal instantons that are absent in [1].

Apart from the above features, we have found a very rich pattern of the zeros of the moduli of the effective Higgs fields χ and ξ, on the branches parametrised by α. These display vortex ring structures described in detail in Section 3, similar to the vortex rings discovered previously [16] in the $3 + 1$ dimensional Yang-Mills–Higgs system.

Acknowledgements

This work is carried out in the framework of Enterprise–Ireland Basic Science Research Project SC/2003/390 of Enterprise-Ireland. The collaboration with Ya. Shnir was supported by a Research Enhancement Grant from the Office of the Dean of Research and Postgraduate Studies of the NUI Maynooth.

References

[1] E. Radu and D. H. Tchrakian, Phys. Lett. B **636** (2006) 201 [arXiv:hep-th/0603071].

[2] A. A. Belavin, A. M. Polyakov, A. S. Shvarts and Y. S. Tyupkin, Phys. Lett. B **59** (1975) 85.

[3] Y. Brihaye, A. Chakrabarti, B. Hartmann and D. H. Tchrakian, Phys. Lett. B **561** (2003) 161 [arXiv:hep-th/0212288].

[4] Y. Brihaye, A. Chakrabarti and D. H. Tchrakian, Class. Quant. Grav. **20** (2003) 2765 [arXiv:hep-th/0202141].

[5] P. Breitenlohner, D. Maison and D. H. Tchrakian, Class. Quant. Grav. **22** (2005) 5201 [arXiv:gr-qc/0508027].

[6] E. Radu and D. H. Tchrakian, Phys. Rev. D **73** (2006) 024006 [arXiv:gr-qc/0508033].

[7] Y. Brihaye, E. Radu and D. H. Tchrakian, arXiv:gr-qc/0610087.

[8] E. Radu, C. Stelea and D. H. Tchrakian, Phys. Rev. D **73** (2006) 084015 [arXiv:gr-qc/0601098].

[9] D. Maison, Commun. Math. Phys. **258** (2005) 657 [arXiv:gr-qc/0405052].

[10] E. Witten, Phys. Rev. Lett. **38** (1977) 121.

[11] C. Rebbi and P. Rossi, Phys. Rev. D **22** (1980) 2010.

[12] D. H. Tchrakian, Phys. Lett. B **150** (1985) 360.

[13] W. Schönauer and R. Weiß, J. Comput. Appl. Math. **27**, 279 (1989);
M. Schauder, R. Weiß and W. Schönauer, *The CADSOL Program Package*, Universität Karlsruhe, Interner Bericht Nr. 46/92 (1992);
W. Schönauer and E. Schnepf, ACM Trans. on Math. Soft. **13**, 333 (1987).

[14] Y. Brihaye, Commun. Math. Phys. **86** (1982) 509.

[15] Y. Brihaye and J. Kunz, J. Math. Phys. **30** (1989) 1913.

[16] B. Kleihaus, J. Kunz and Y. Shnir, Phys. Lett. B **570** (2003) 237 [arXiv:hep-th/0307110];
B. Kleihaus, J. Kunz and Y. Shnir, Phys. Rev. D **68** (2003) 101701 [arXiv:hep-th/0307215];
B. Kleihaus, J. Kunz and Y. Shnir, Phys. Rev. D **70** (2004) 065010 [arXiv:hep-th/0405169].

[17] B. Kleihaus, J. Kunz and Y. Shnir, Phys. Rev. D **71** (2005) 024013 [arXiv:gr-qc/0411106].

[18] Y. Brihaye, E. Radu and D. H. Tchrakian, Int. J. Mod. Phys. A **19** (2004) 5085 [arXiv:hep-th/0405255].

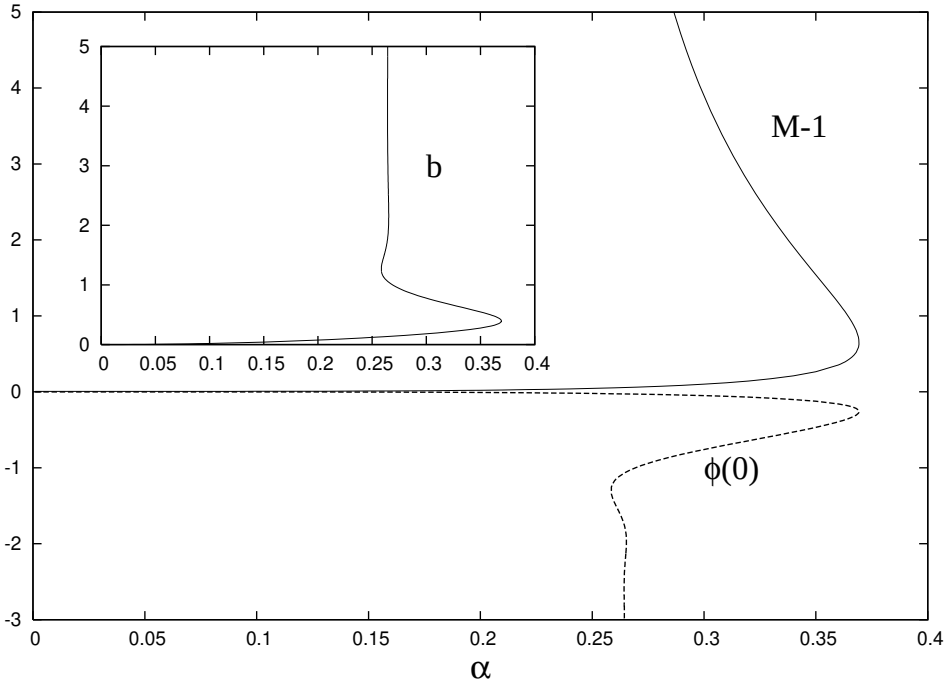

Figure 1. The mass M, the shooting parameter b and the value of the dilaton at the origin $\phi(0)$ are shown as a function of α for $n = 1,\ m = 1$ spherically symmetric YMd solutions. (Here and in Figure 2, we use a normalization such that the mass of $\alpha = 0$ self-dual $p = 1$ YM solutions is $M = q = n^2$.)

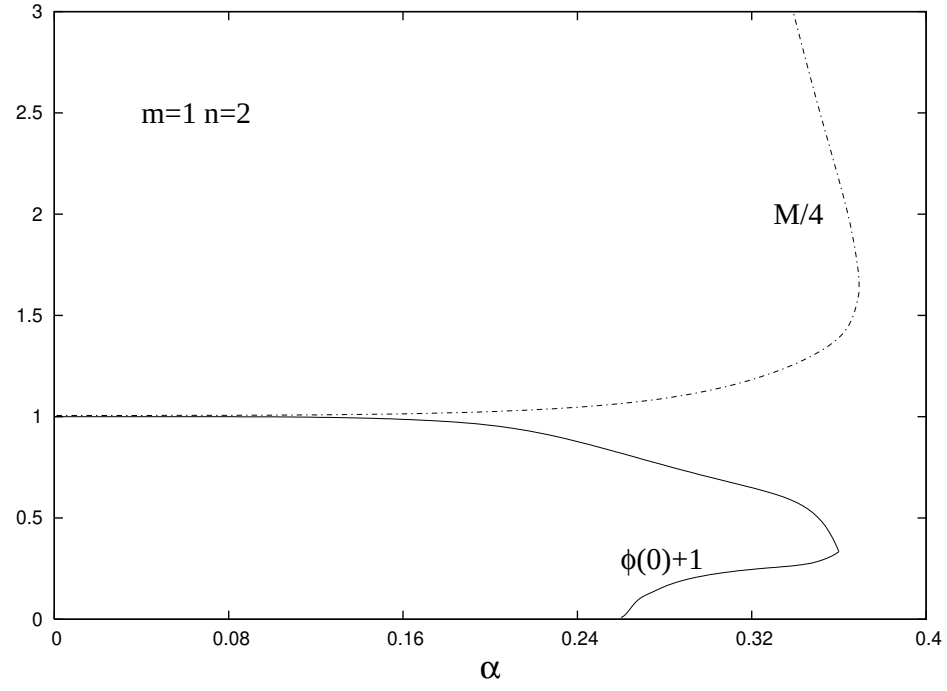

Figure 2. The mass M and the value of the dilaton field at the origin $\phi(0)$ are shown as a function of α for $n = 1,\ m = 2$ YMd solutions.

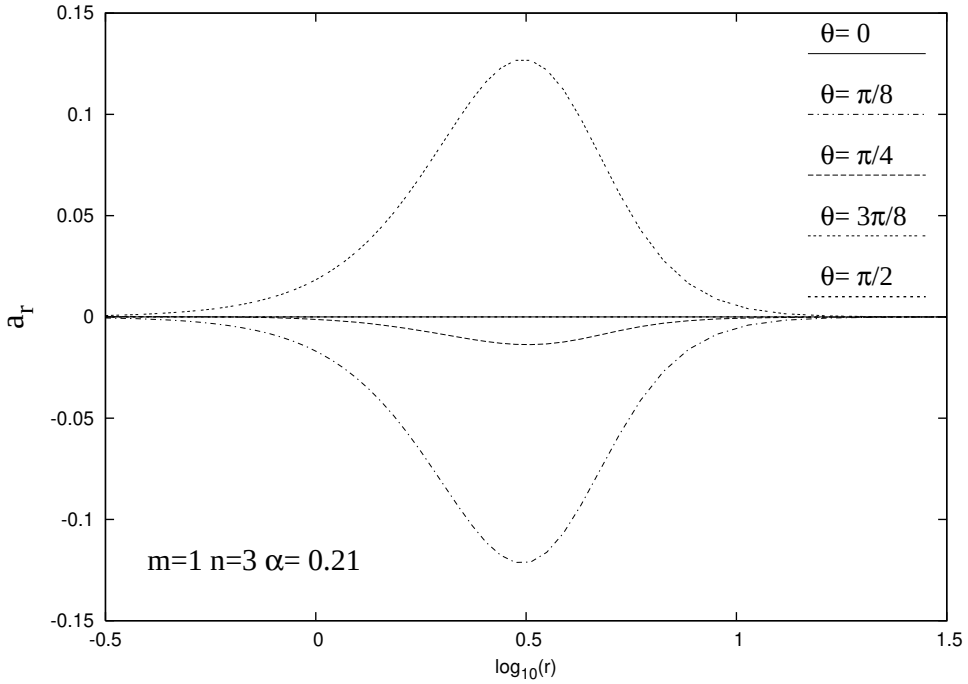

Figure 3a.

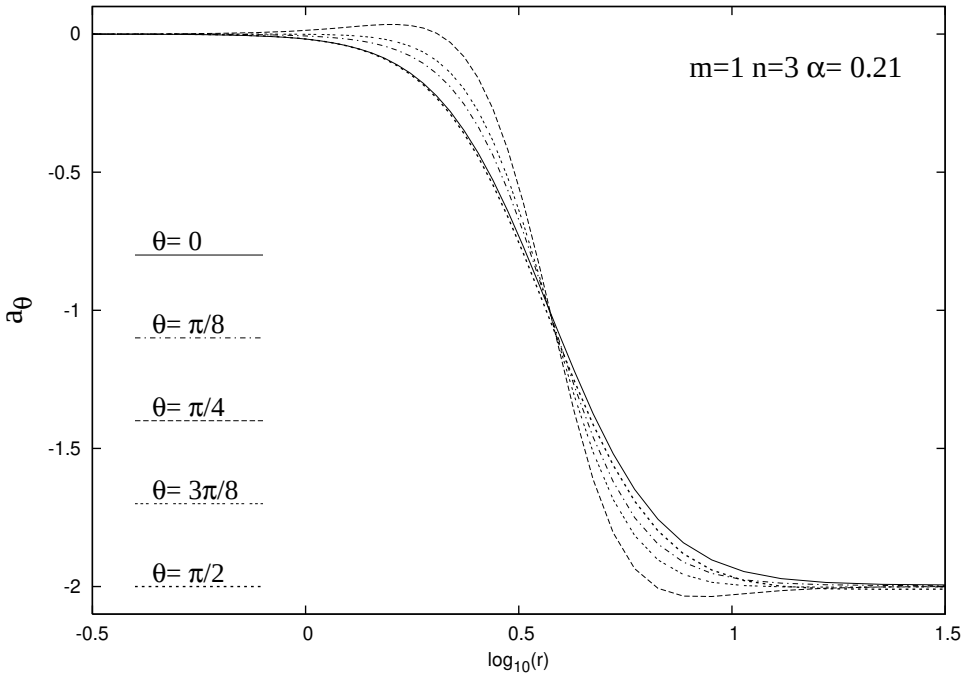

Figure 3b.

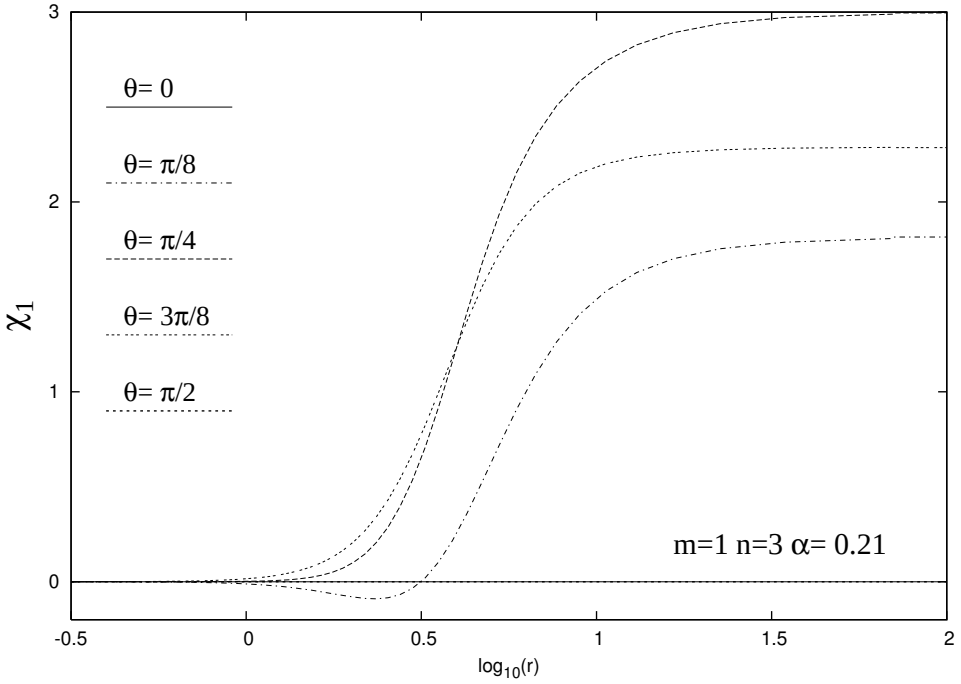

Figure 3c.

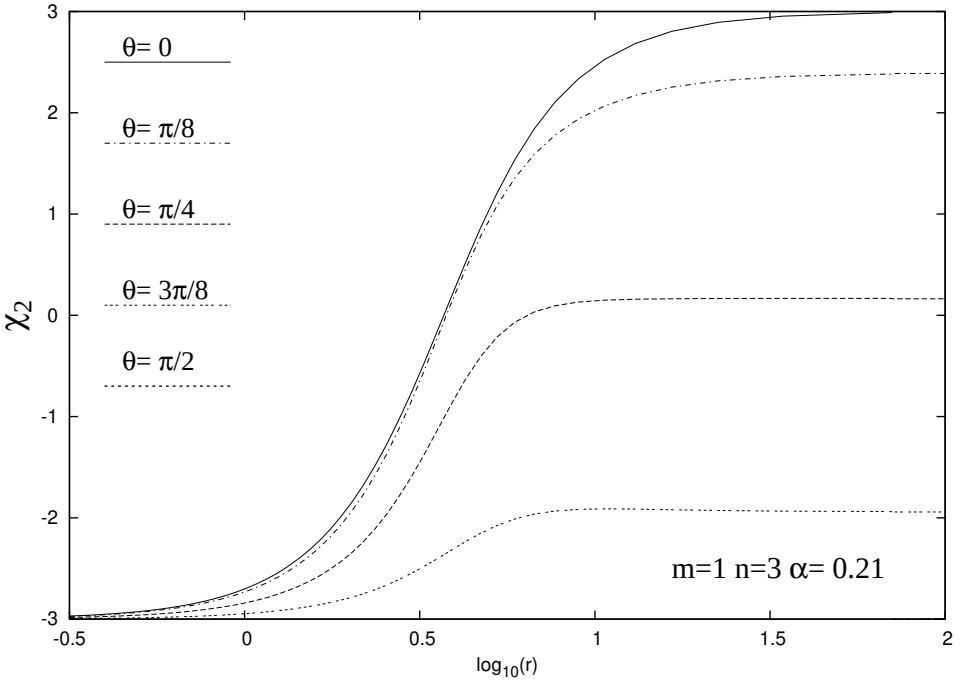

Figure 3d.

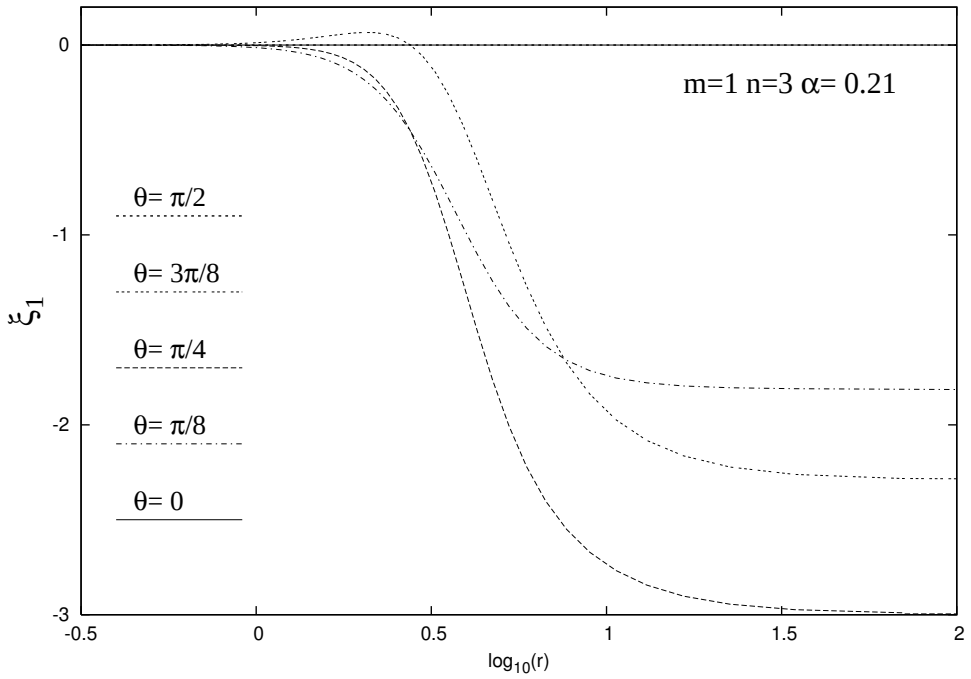

Figure 3e.

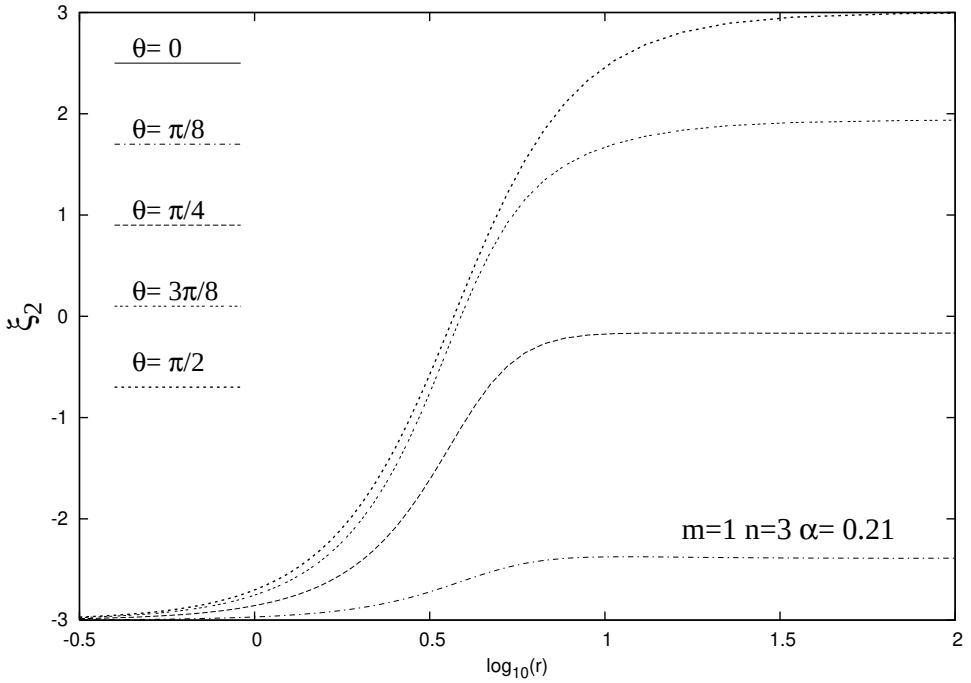

Figure 3f.

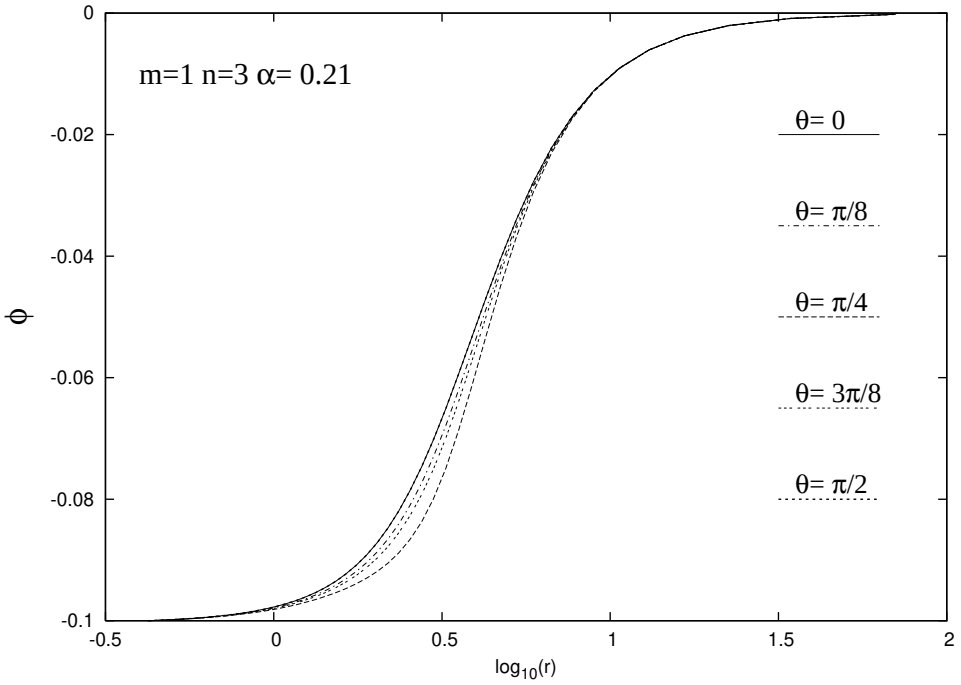

Figure 3g.

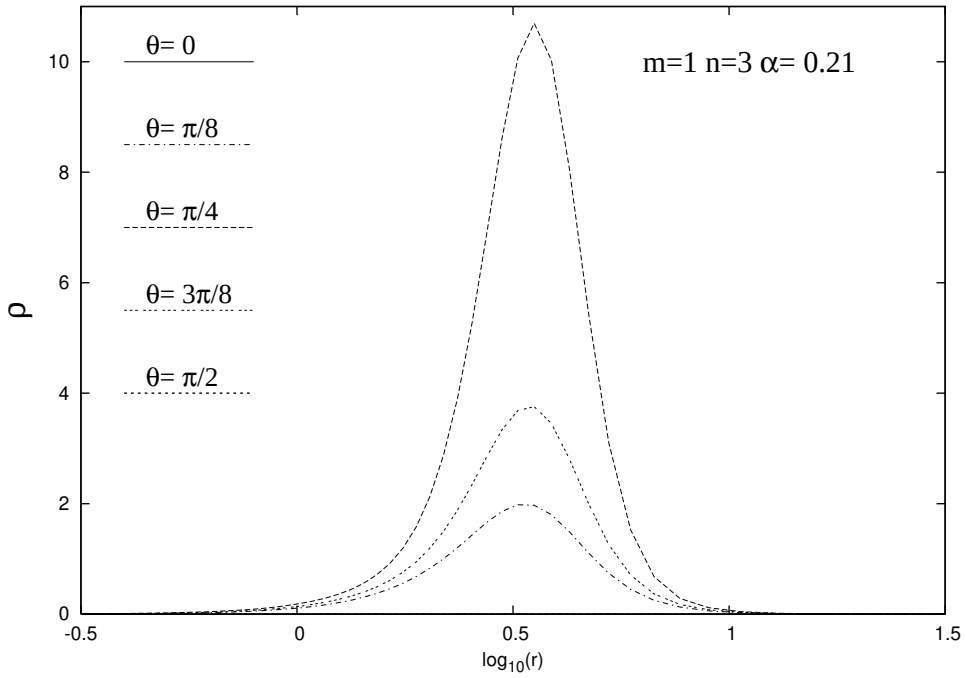

Figure 3h. The YM gauge functions, the dilaton field and the topological charge density ρ are shown as a function of the radial coordinate r for a typical $m = 1,\ n = 3$ YMd solutions with $\alpha = 0.21$.

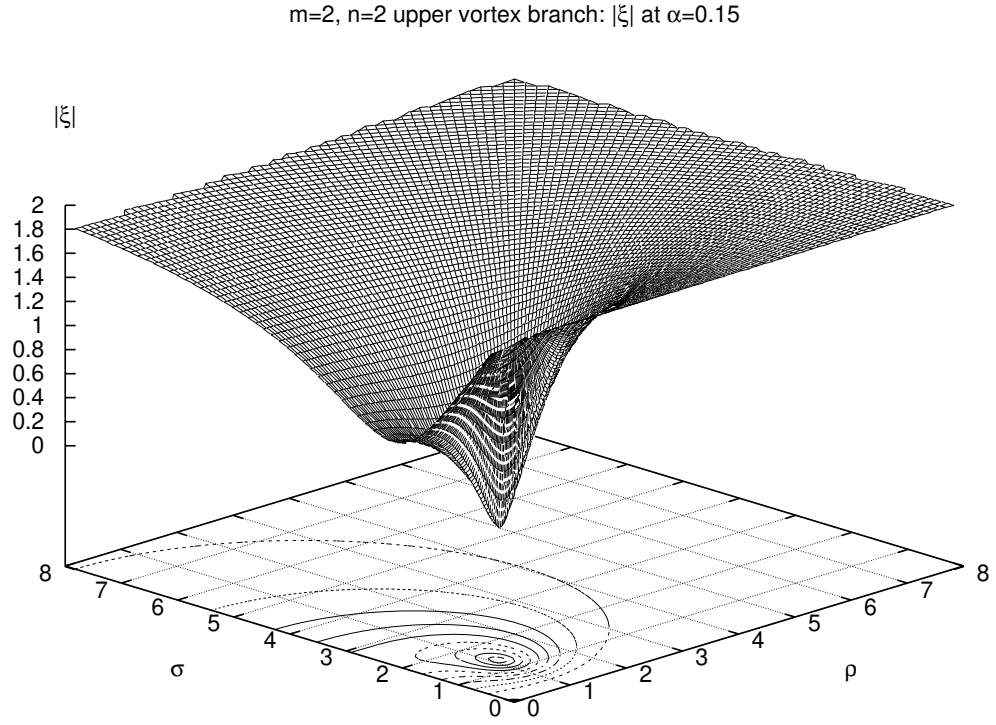

Figure 4a.

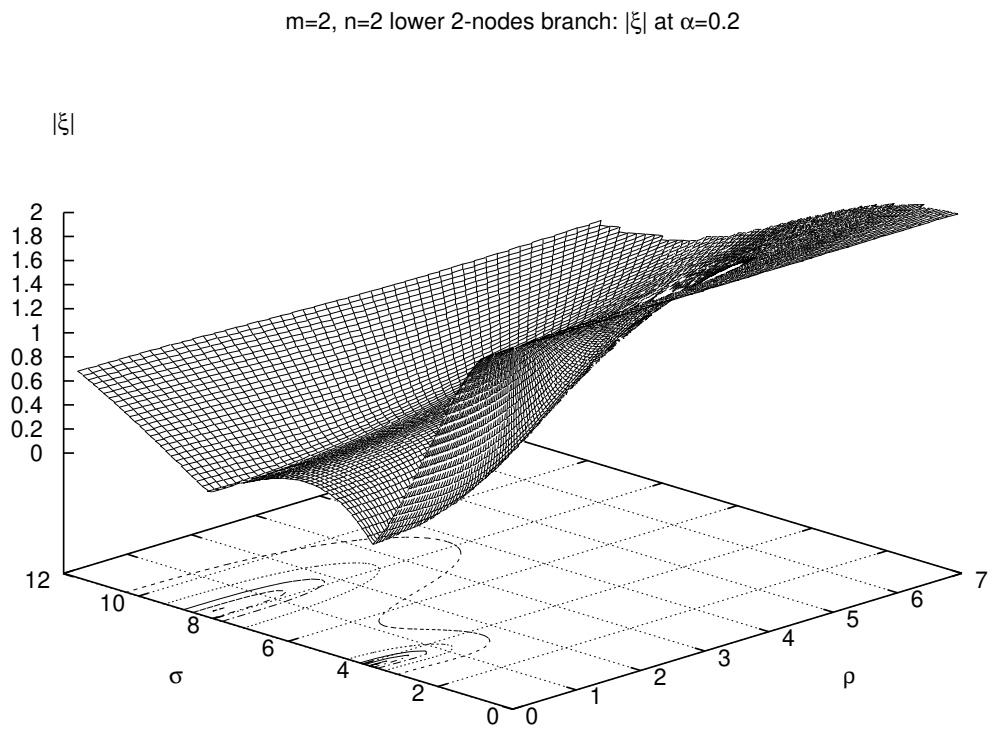

Figure 4b.

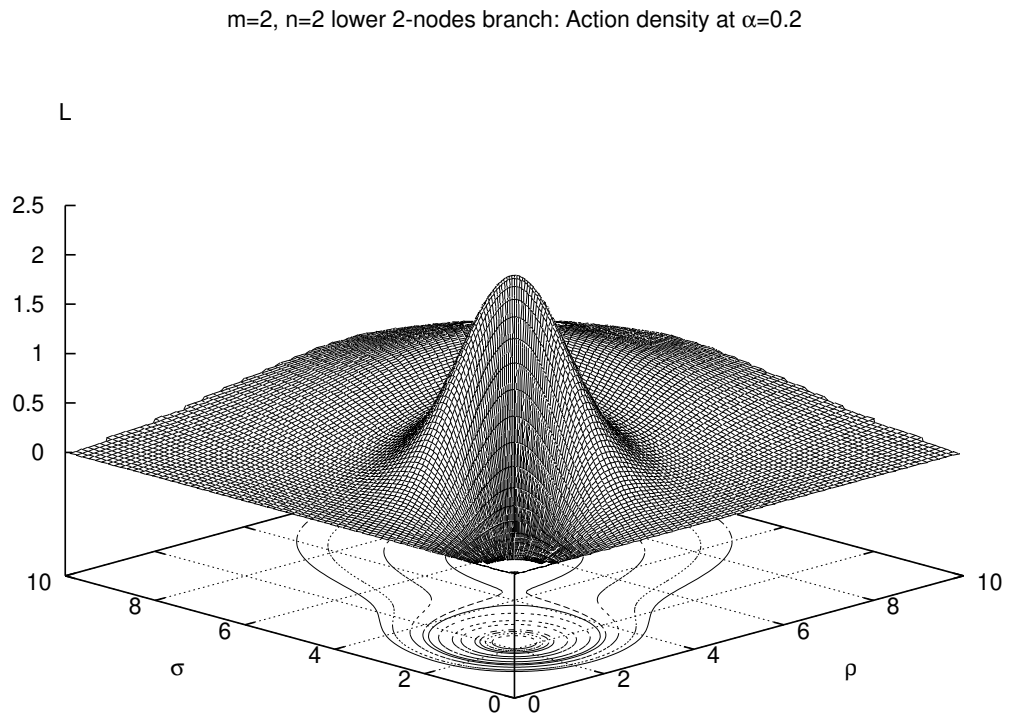

Figure 4c.

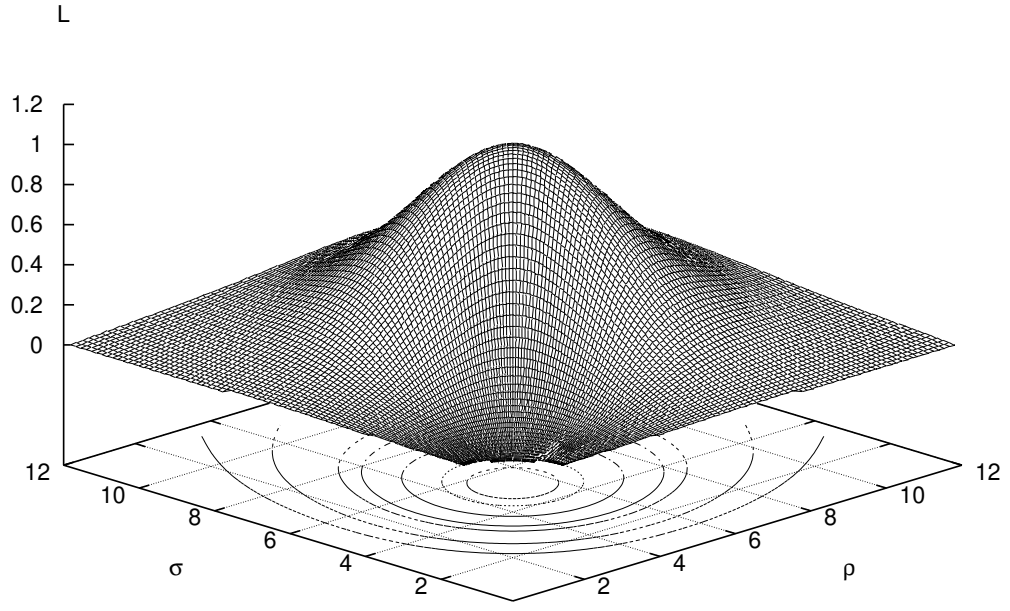

Figure 4d. The modulus of the effective Higgs field ξ is shown for the uper branch $m = 2, n = 2$ solutions at $\alpha = 0.15$ (vortex, Figure 4a) and $\alpha = 0.20$ lower energy branch solution (double node, Figure 4b) as functions of the coordinates ρ and σ. The action density distributions of these $m = 2, n = 2$ solutions at $\alpha = 0.20$ are also shown on the lower branch (Figure 4c) and on the upper branch (Figure 4d), respectively.

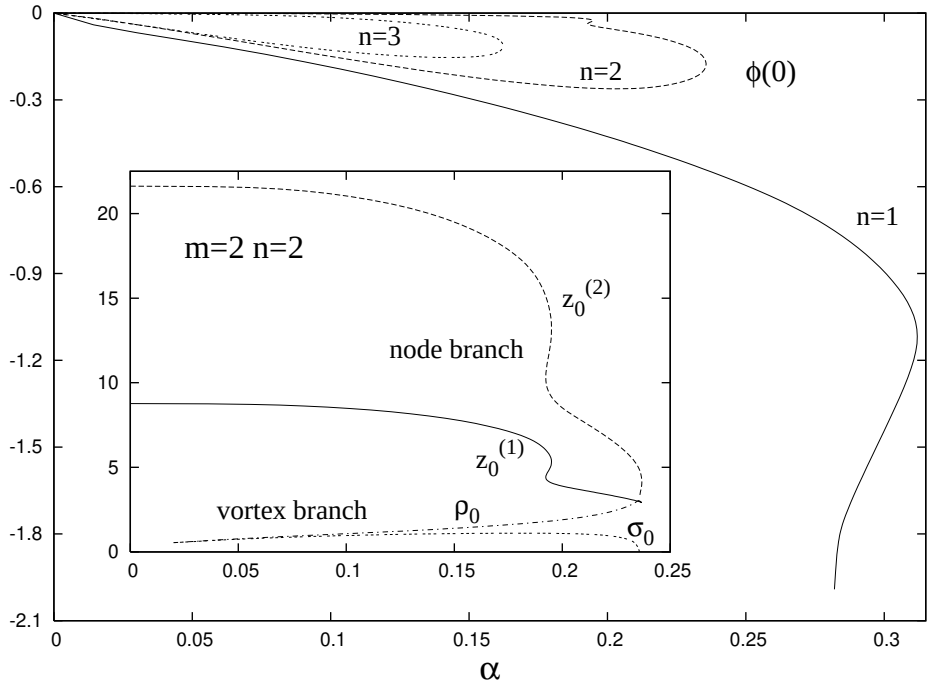

Figure 5a.

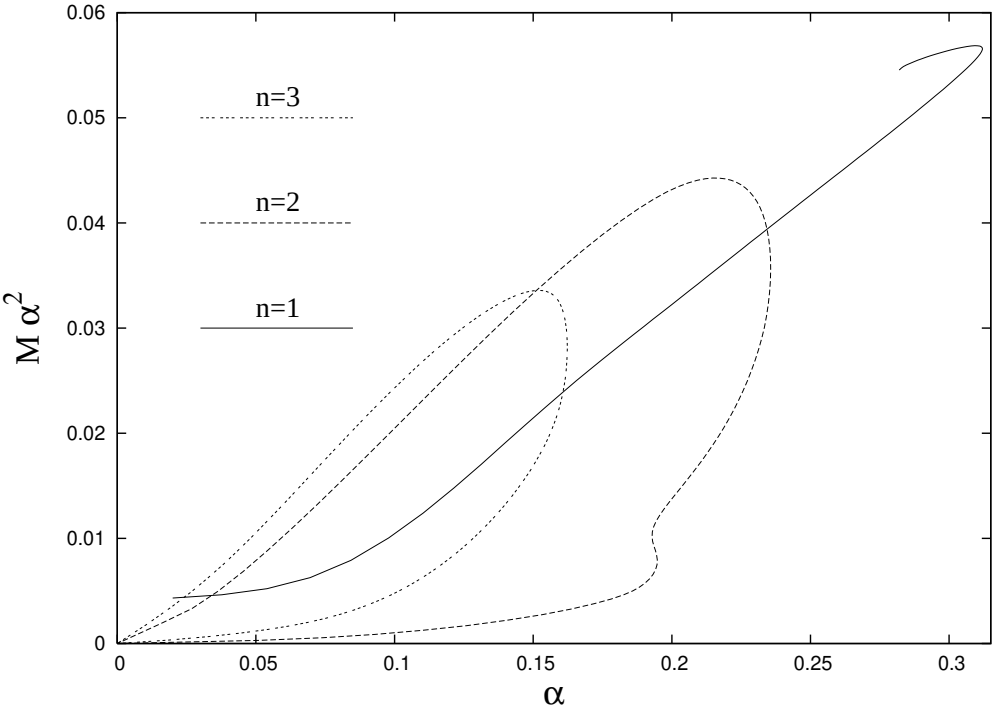

Figure 5b. The values of the dilaton function ϕ at the origin (Figure 5a) and the unrescaled mass $M\alpha^2$ (Figure 5b) of the configuration with $m = 2,\ n = 1, 2, 3$ are shown as functions of the effective coupling constant α. The location of the vortices as given by (ρ_0, σ_0) and the position of nodes $(z_0^{(1)},\ z_0^{(2)})$ is also presented in Figure 5a for $m = 2,\ n = 2$ solutions.

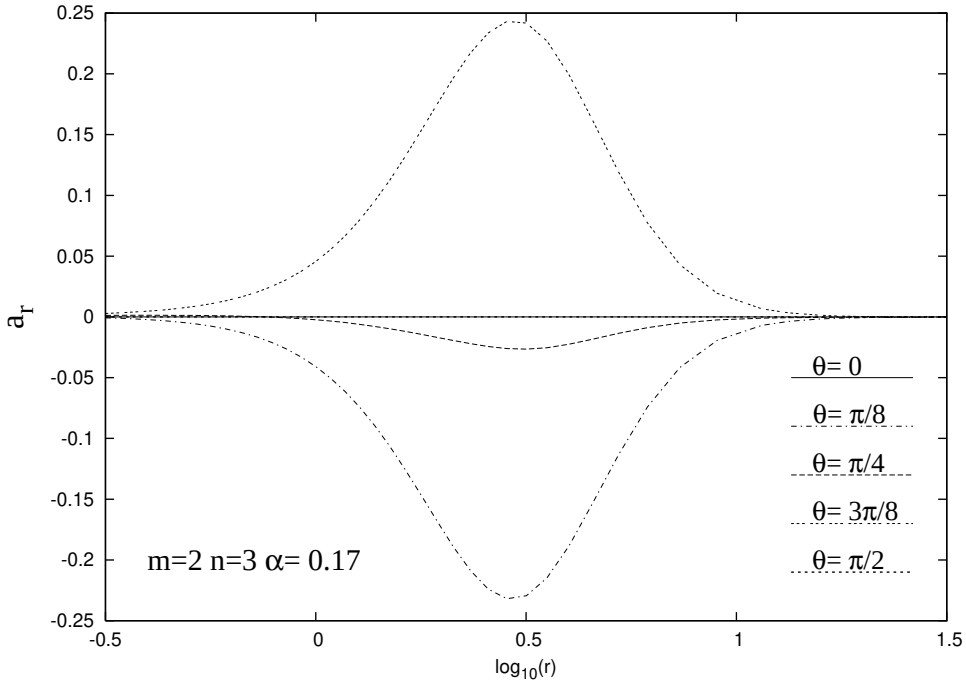

Figure 6a.

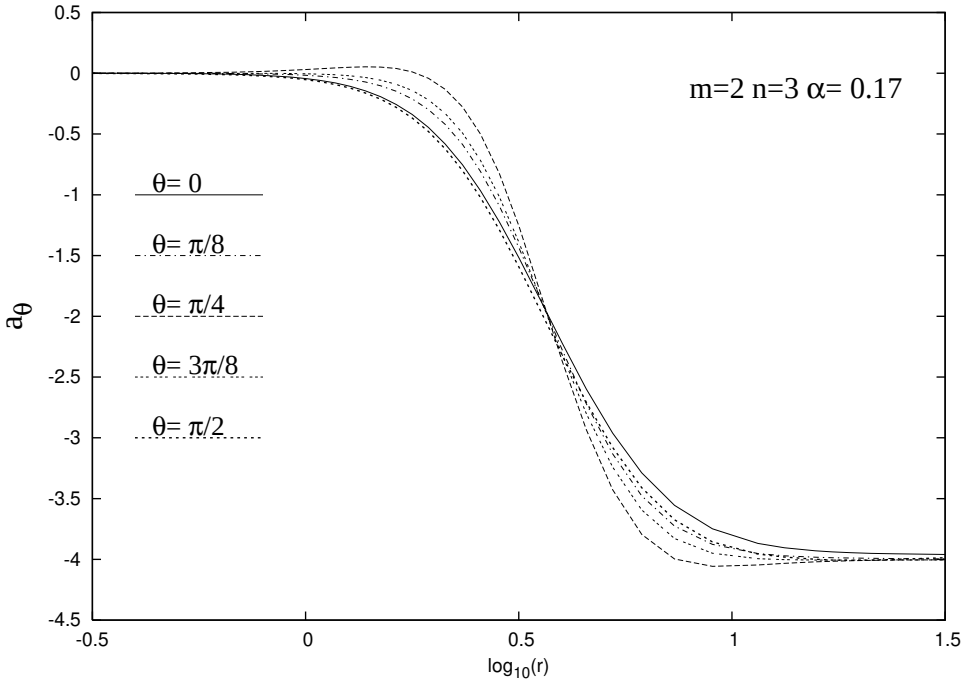

Figure 6b.

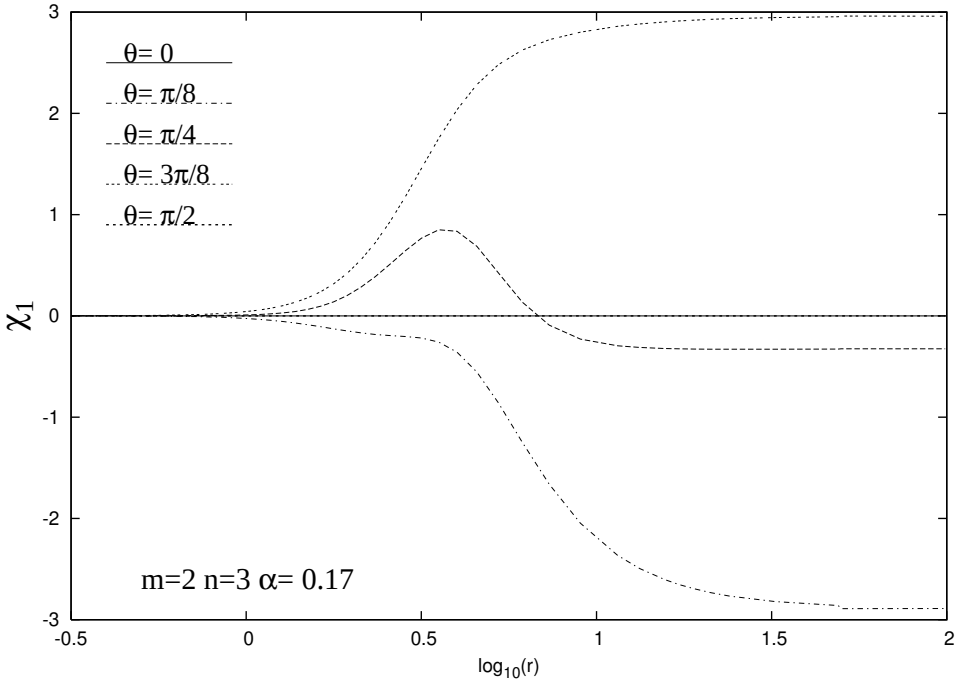

Figure 6c.

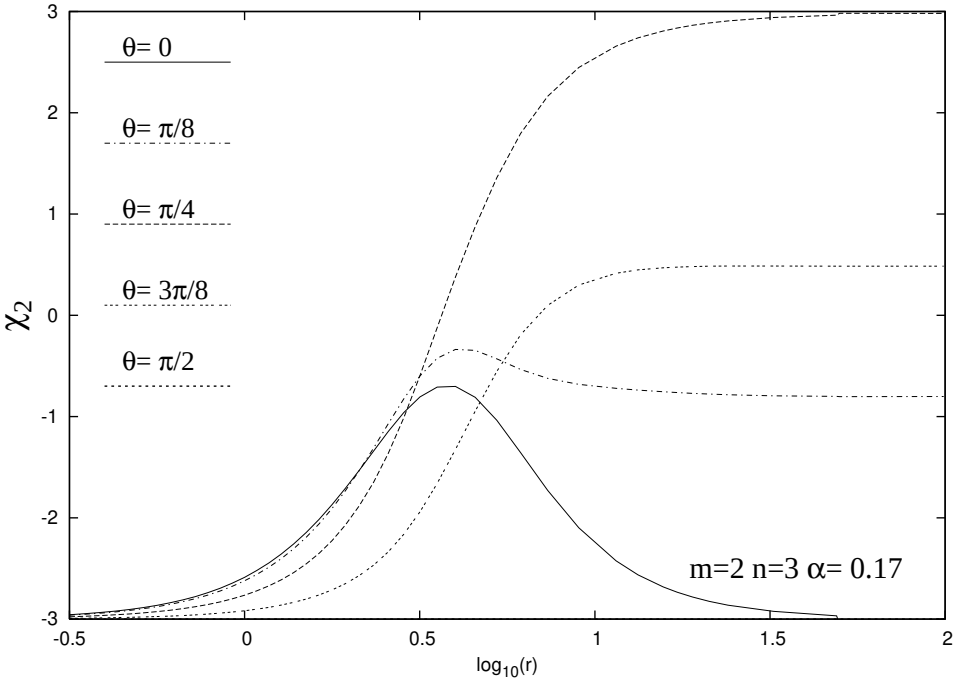

Figure 6d.

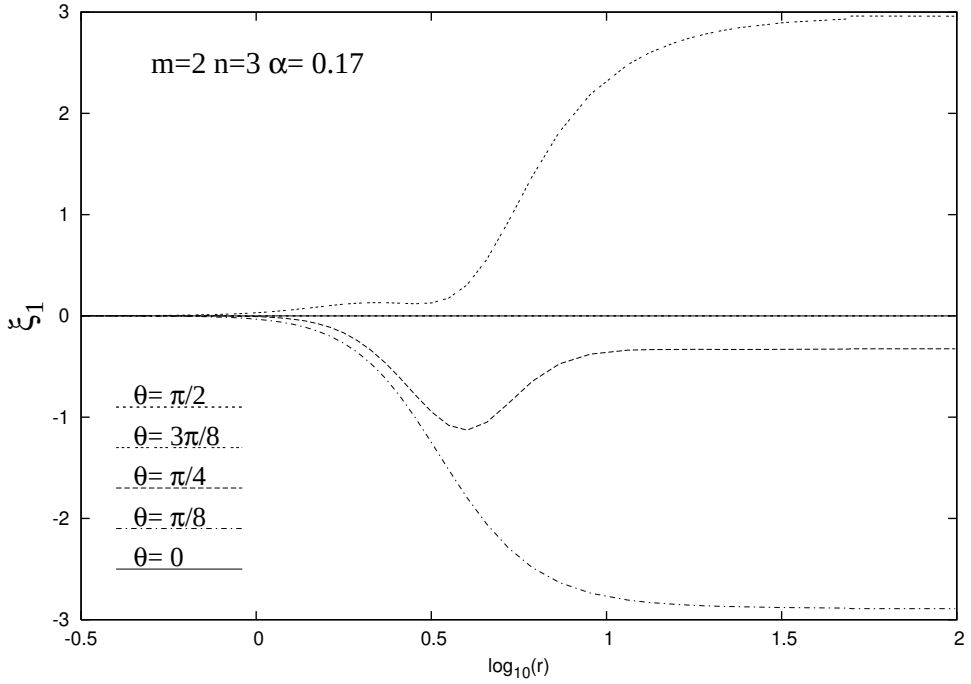

Figure 6e.

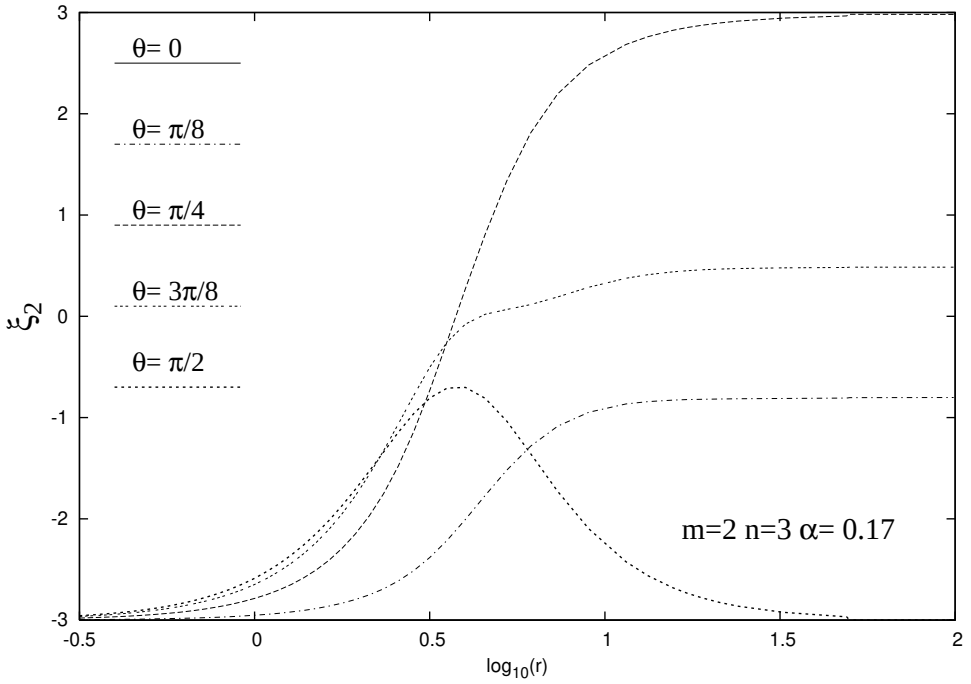

Figure 6f.

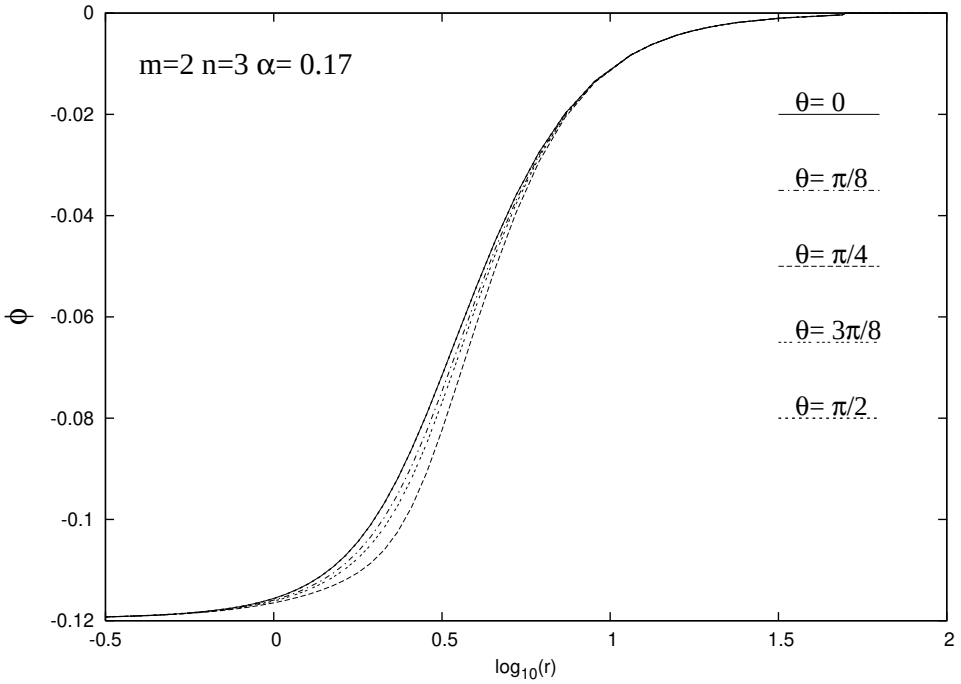

Figure 6g. The YM gauge functions and the dilaton field are shown as a function of the radial coordinate r for a typical $m = 2,\ n = 3$ YMd solutions with $\alpha = 0.17$.